

Multiphoton Femtosecond Coherent Control in the Single-Cycle Regime

Lev Chuntunov, Avner Fleischer, and Zohar Amitay*

Schulich Faculty of Chemistry, Technion - Israel Institute of Technology, Haifa 32000, Israel

Coherent control of the atomic two-photon absorption with shaped single-cycle pulses is examined theoretically in the weak-field regime. The control over the stabilized carrier-envelope phase (CEP) of the pulses is determined as a key parameter allowing the full utilization of the ultrabroad pulse spectrum. This bandwidth is sufficient to provide besides the sequential two-photon pathways, additional Raman-type pathways coupling between the ground and the excited states. The interference between the different pathways is efficiently controlled via the control over the CEP. Simplified two-level model is analyzed in the frequency domain where the rational pulse shaping is applied. The developed intuition is applied to atomic Cs and verified by the exact numerical solution of time-dependent Schrödinger equation.

PACS numbers: 32.80.Qk, 32.80.Wr, 42.65.Dr

Ultrashort laser pulses are a unique experimental tool to explore and control the ultrafast dynamics of the quantum systems [1, 2, 3, 4, 5, 6, 7, 8, 9, 10, 11]. The ultrashort duration of the pulses is originated from their ultrabroad coherent spectral bandwidth which provides a manifold of photoinduced multiphoton pathways between the ground and the excited states of the system. The relative phase, amplitude, and polarization of different pulse spectral components are used to manipulate the interference between the pathways. These characteristics are assigned to the spectral components using pulse shaping techniques [22] and act as control parameters for enhancing or attenuation of the transition probability to the excited state. In particular, shaped femtosecond pulses are extensively used for experimental coherent control of bound-bound multiphoton transitions in atoms and molecules at different regimes of the excitation pulse intensities [3, 4, 5, 6, 7, 8, 9, 10, 11]. Recently, the pulses as short as few optical cycles became widely available [12, 13, 14, 15, 16]. One of the basic characteristics of the few-cycle pulses is the relative phase between the spectral components of the pulse and its spectral envelope. In the time-domain, this global phase is translated to the relative phase between the carrier wave of the pulse and its temporal envelope. Carrier-envelope phase (CEP) plays significant role in the many multiphoton processes like photoionization in the various pulse-intensity regimes, high harmonics generation, and others [16, 17, 18, 19, 20, 21]. It is also a very important parameter to be considered for the coherent control of bound-bound multiphoton transitions with the single-cycle pulses. In the present work we demonstrate the role of the CEP on the multiphoton absorption in the weak-field limit. We show that CEP stabilization is necessary to obtain full control over the multiphoton excitation when single-cycle pulses are used. The tunable values of CEP also serve as an additional control knob in that process. The control of the population transfer to

the excited state of the system (i.e. degree of multiphoton absorption) is demonstrated first on the simplified two-level model and then applied to the atomic caesium (Cs).

Although the ultrashort duration of the single-cycle pulses suggests the inspection of the associated phenomena in the time-domain, in many cases, especially in the range of weak- to intermediate- pulse intensities [3, 4, 5, 6, 7, 8, 9], frequency-domain analysis provides is preferable. As frequency domain is a domain where the actual pulse shaping is applied, it is also the domain of the powerful rational pulse design, which is based on the identification of the photoinduced multiphoton pathways, once the complete photo-excitation picture of the system is available. The typical bandwidth of the pulses used in the recent control experiments is 30-50nm (fwhm), corresponding to the shortest possible pulse duration of 20-30fs (transform-limited pulse). The spectral components available within this bandwidth contribute to the pathways with the single possible combination of the number of absorbed and emitted photons. For example for the two-photon absorption process, such combination is the sequential absorption of two photons, while for the Raman process it is absorption of one photon and emission of one photon. Consequently, all the corresponding two-photon pathways in both cases have the same global phase, associated with CEP, and their interference does not depend on its specific value.

Recently, the shaped pulses with octave spanning bandwidth became available [23]. The shaped single-cycle pulses are expected to emerge in the nearest future. Their ultrabroad bandwidth provides additional types of pathways between the ground and the excited states of the system to be used for the control over the multiphoton absorption. As such, there are several possible combinations of the number of absorbed and emitted photons contributing to the different types of pathways. However, as it is shown below, the full control over their interference is only possible for the pulses with stabilized CEP. For example, consider the excitation of the system from the ground state $|g\rangle$ of energy E_g to the excited state $|f\rangle$ of energy E_f which can be accessed with

*Electronic address: amitayz@tx.technion.ac.il

the absorption of two photons with frequencies that sum up to the two-photon resonance $\Omega_{fg} = (E_f - E_g)/\hbar$: $\Omega_{fg} = \omega_{seq} + \omega'_{seq}$, where $\Omega_{fg} > \omega_{seq}, \omega'_{seq}$. In addition, the octave-spanning spectrum provides the Raman-type pathways [6, 7, 8] that lead to the same excited state with absorption of one and emission of one photon. The frequencies of the photons sums up to the two-photon transition $\Omega_{fg} = \omega_{Ram} - \omega'_{Ram}$, where $\omega_{Ram} > \Omega_{fg} > \omega'_{Ram}$. The ground and the excited states of the system are coupled via the manifold of the intermediate states $|n\rangle$ that for the case of non-resonant two-photon absorption are not accessible by the one-photon process.

The total amplitude of the excited state $A_f^{(2)}$ is proportional to the Fourier transform of the square electric field of the laser pulse

$$A_f^{(2)} \propto \int_{-\infty}^{\infty} E^2(t) \exp[i\Omega_f t] dt, \quad (1)$$

where

$$E(t) = \frac{1}{2} \mathcal{E}(t) \exp[i(\omega_0 t + \phi_{CE})] + C.C., \quad (2)$$

$\mathcal{E}(t)$ - is gaussian temporal complex amplitude of the pulse, ω_0 - is the carrier frequency, ϕ_{CE} - is the CEP, and $C.C.$ stands for the complex conjugate term. The electric field of the pulse $E(t)$ corresponds to the spectral field $E(\omega) = \mathcal{E}(\omega) \exp[i\phi_{CE}] + C.C.$, where $\mathcal{E}(\omega)$ - is the spectral complex envelope of the pulse $\mathcal{E}(\omega) = |\mathcal{E}(\omega)| \exp[i\Phi(\omega)]$, $|\mathcal{E}(\omega)|$ - is the spectral amplitude, and $\Phi(\omega)$ is the relative spectral phase. The shortest possible pulse for a given spectrum, referred as transform-limited (TL) pulse, corresponds to $\Phi(\omega) \equiv 0$ for any ω . The global phase ϕ_{CE} modifies the exact temporal shape of the pulse, but not affects its duration. The excited state population $P_f = |A_f^{(2)}|^2$ is expressed in the frequency domain as a summation over the amplitudes contributed by the sequential $A_S^{(2)}$ and the Raman $A_R^{(2)}$ types of pathways

$$P_f = \left| \mu_{seq}^2 A_S^{(2)}(\Omega_f) + \mu_{Ram}^2 A_R^{(2)}(\Omega_f) \right|^2, \quad (3)$$

where μ_{seq}^2 and μ_{Ram}^2 are effective non-resonant two-photon sequential and Raman transitional dipole moments correspondingly, and

$$A_S^{(2)}(\Omega) = \exp[i2\phi_{CE}] \int_0^\infty \mathcal{E}(\omega) \mathcal{E}(\Omega - \omega) d\omega \quad (4)$$

$$A_R^{(2)}(\Omega) = 2 \int_\Omega^\infty \mathcal{E}(\omega) \mathcal{E}^*(\omega - \Omega) d\omega$$

For the pulse with stabilized CEP equals ϕ_{CE} these two types of pathways have relative phase of $\Delta\phi = 2\phi_{CE}$, which dictates the nature of the interference between them.

Consider the model quantum system with two-photon transition of $\Omega_f = 12500 \text{cm}^{-1}$. The sequential and Raman types of pathways are shown schematically on Figure 1(a). The duration of the pulse with fwhm equals

to one optical cycle of its carrier frequency of $\omega_0 = 12500 \text{cm}^{-1}$ (800nm) is 2.7fs, and the corresponding spectral width of such pulse is 5425cm^{-1} . The typical spectrum of the pulse and its temporal electric field are drawn on Figure 1(b) and (c), respectively. As opposed to the case of the two-photon absorption with pulses of narrower spectrum, where the considered optimal spectrum is centered at the half of the two-photon transition $\omega_0 = \Omega_f/2$, in the case of single-cycle pulse in order to utilize the interference between different types of pathways the spectrum of the pulse should be centered near Ω_f . This spectral positions ensures that the pairs of photons around $\Omega_f/2$ contributing to the sequential type of pathways, as well as the pairs of photons consisted of one $3\Omega_f/2$ -photon and one $\Omega_f/2$ -photon contributing to Raman type of pathways are provided. The relative weight of each type of pathways is set on one hand by the corresponding values of the effective two-photon transitional dipole moments μ_{seq}^2 and μ_{Ram}^2 , and on the other hand by the spectral amplitude profile of the pulse. In our model system we set $\mu_{seq}^2 = \mu_{Ram}^2$ for simplicity.

We examine now the dependence of the transition probability to the excited state on the value of ϕ_{CE} . The electric field of the pulses with different ϕ_{CE} is shown on Figure 1(b). In the frequency domain these pulses correspond to different global spectral phase. The beating of the excited state population against the ϕ_{CE} is traced on Figure 1(d) for different ω_0 . Each trace is normalized to the case of $\phi_{CE} = 0$, where the maximum of the pulse electric field oscillations coincides with the maximum of the envelope. The amplitudes $A_S^{(2)}$ and $A_R^{(2)}$ are in phase in this case and interfere constructively. Their relative weight depends on the spectral position, and determines the maximum of the modulation depth $M = 2 \frac{\max(P_f) - \min(P_f)}{\max(P_f) + \min(P_f)}$. Therefore, we have $M_{\phi_{CE}=0} = 0$. As it is shown on Figure 1(d), the maximal values of M are obtained for the case of $\phi_{CE} = \pi/2$. When the spectrum is shifted to the higher frequencies, the relative weight of the Raman pathways dominates the sequential ones, while when the spectrum is shifted to the lower frequencies - sequential pathways dominate. The higher is the difference in the relative amplitudes, the lower is the modulation depth M . The maximal contrast in the modulation depth $M_{\phi_{CE}=\pi/2} = 2$ was achieved for $\omega_0 = 11870 \text{cm}^{-1}$ [Figure 1(d), thick solid line], corresponding to the red shift of the spectrum as compared to the two-photon resonance $\Omega_f = 12500 \text{cm}^{-1}$.

Next, as a test-case for the coherent control of two-photon absorption, we consider the phase-shaped pulses, having a π -step spectral phase pattern, while the step position ω_{step} is scanned along the pulse spectrum. The control of the excited state population is examined for the pulses with different positions of the spectrum [different ω_0], and the results are plotted on Figure 2. For each spectrum we show the traces of the excited state population as a function of ω_{step} for $\phi_{CE} = 0$, $\phi_{CE} = \pi/2$, and the trace averaged over all possible values of ϕ_{CE} .

The latter corresponds to the case of the not stabilized CEP. The calculated results are normalized to the population excited by the unshaped pulse with $\phi_{CE}=0$. The results strongly emphasize the role of the CEP stabilization of the few-cycle pulses and the dependence of the excitation yield on the actual value of ϕ_{CE} . The case of $\omega_0 = 11870\text{cm}^{-1}$ is shown on panel (b). For the pulse with ω_{step} at the very low frequencies the excited population is the same as shown on Figure 1(d). When ω_{step} is set at the high frequency region, all the spectrum experience additional constant phase of π . Here the global phase of the shaped pulses has been changed from $\phi_{CE} = 0$ and $\phi_{CE} = \pi/2$ to $\phi_{CE} = \pi$ and $\phi_{CE} = 3\pi/2$, however, the excitation yields remain the same as can be expected from Figure 1(d).

The picture is different when the ω_{step} is set in the middle of the spectrum. Take for example $\omega_{step} = 12500\text{cm}^{-1}$ with $\phi_{CE} = 0$. The spectral components near $\Omega_f/2$ of the sequential two-photon pathways have zero relative phase and interfere constructively within $A_S^{(2)}(\Omega_f)$. The spectral components of the Raman pathways has different phases [0 for $\omega < \omega_{step}$ and π for $\omega \geq \omega_{step}$] as they are coming from the different spectral regions. Consequently, the Raman pathways interfere constructively within $A_R^{(2)}(\Omega_f)$, but there is a global phase of π between the amplitudes $A_S^{(2)}(\Omega_f)$ and $A_R^{(2)}(\Omega_f)$. Hence, while for the unshaped pulse $\phi_{CE} = 0$ corresponds to the completely constructive interference between $A_S^{(2)}(\Omega_f)$ and $A_R^{(2)}(\Omega_f)$, for the shaped pulse with $\omega_{step} = 12500\text{cm}^{-1}$ the interference is completely destructive and the overall excited state population is zero. When the similar analysis is applied to the case of $\phi_{CE} = \pi/2$, we obtain that while for the unshaped pulse the excited population is zero due to the destructive intergroup interference, it is turned into the constructive one by the corresponding pulse shaping with $\omega_{step} = 12500\text{cm}^{-1}$.

Our two-state frequency domain perturbative model is verified here by the exact solution of the time-dependent Schrödinger equation for the atomic Cs irradiated by the shaped single-cycle pulses. We used numerical propagation by fourth-order Runge-Kutta method. The 6s state was considered as the ground state, while the $5d_{3/2}$ and $5d_{5/2}$ states – as the excited states. The excitation scheme is shown on Figure 3: the sequential pathways are drawn by the solid line, the Raman pathways – by the dashed line. The two-photon coupling between the ground and excited states is provided by the manifold of the p-states of the atom. Overall, we have considered 6s-9s, 6p-8p, and 5d-7d states, including also their fine structure splitting. The information on the atomic levels and the corresponding transitional dipole moments can

be found in [24, 25, 26, 27]. As opposed to our two-state model, in real atom the values of the effective two-photon transition dipole moments are generally not equal in magnitude, and also can have different sign, depending on the specific atomic structure. Here we first examine the dependence of the final states population on the ϕ_{CE} value of the excitation pulse, and then demonstrate the results for the shaped pulses.

The energies of the $5d_{3/2}$ and $5d_{5/2}$ states are $\Omega_{f1}=14499.3\text{cm}^{-1}$ and $\Omega_{f2}=14596.8\text{cm}^{-1}$, respectively. We have found that control of the excited population is most efficient when the spectrum of the pulse is centered at $\omega_0=16667\text{cm}^{-1}$ [600nm]. The optical cycle corresponding to this wavelength has duration of 2fs, and the bandwidth associated with the single-cycle pulse is 7350cm^{-1} . The calculated results are shown on Figure 3(a),(b). The maximal modulation value $M=2$ for the $5d_{5/2}$ -state population is obtained with $\phi_{CE}=3.3\text{rad}$. For the $5d_{3/2}$ state the maximal modulation value obtained is $M=1.7$ corresponding to $\phi_{CE} = 3.3$.

On Figure 3(c),(d) we demonstrate results for the excitation of Cs atoms for the case of $\phi_{CE}=3.3$ for various π -step positions. When $\omega_{step} = \omega_0$, as it was expected from the analysis of the two-level system, the destructive interference between the sequential and the Raman pathways is turned into the constructive one, and the two-photon absorption for such shaped pulses is maximal for a given spectrum. The two-photon excitation process of Cs with broadband spectrum at $\omega_0=16667\text{cm}^{-1}$ has resonance-mediated nature [5]. It is reflected in the response to the excitation with π -step phase shaped pulses. When the ω_{step} is set exactly at the frequency corresponding to initial-to-intermediate or intermediate-to-final state resonance transition, there is a significant enhancement in the two-photon absorption. The mechanism of such enhancement is conversion of destructive interference between the sequential two-photon pathways associated with the TL pulse into constructive one by the appropriate pulse shaping [5]. Consequently, each peak in the two-photon absorption that appear on Figure 3(c),(d) correspond to the specific resonance of the system.

To summarize, we have demonstrated coherent control of the two-photon absorption in the single-cycle regime. The important role of the CEP in control over the interference between the sequential and Raman-type pathways is revealed in the frequency domain analysis applied to the two-level model system, extended to atomic Cs, and verified by the exact solution of the time-dependent Schrödinger equation. The results for coherent control of two-photon absorption are compared with the case of non-stabilized CEP.

[1] D. J. Tannor, R. Kosloff, and S. A. Rice, J. Chem. Phys. **85**, 5805 (1986).

[2] M. Shapiro and P. Brumer, *Principles of the quantum*

- control of molecular processes* (Wiley, New Jersey, 2003).
- [3] M. Dantus and V. V. Lozovoy, Chem. Rev. **104**, 1813 (2004); ChemPhysChem **6**, 1970 (2005).
 - [4] D. Meshulach and Y. Silberberg, Nature (London) **396**, 239 (1998); Phys. Rev. A **60**, 1287 (1999).
 - [5] N. Dudovich *et al.*, Phys. Rev. Lett. **86**, 47 (2001).
 - [6] D. Oron *et al.*, Phys. Rev. A **65**, 043408 (2002); N. Dudovich, D. Oron, and Y. Silberberg, Nature (London) **418**, 512 (2002);
 - [7] H. U. Stauffer *et al.*, J. Chem. Phys. **116**, 946 (2002); X. Dai, E. W. Lerch, and S. R. Leone, Phys. Rev. A **73**, 023404 (2006).
 - [8] E. Gershgoren *et al.*, Opt. Lett. **28**, 361 (2003).
 - [9] L. Chuntunov *et al.*, Phys. Rev. A **77**, 021403(R) (2008); J. Phys. B **41**, 035504 (2008).
 - [10] A. Präkelt *et al.*, Phys. Rev. A **70**, 063407 (2004).
 - [11] B. Chatel, J. Degert, and B. Girard, Phys. Rev. A **70**, 053414 (2004).
 - [12] P. Dombi *et al.*, New J. Phys. **6**, 39 (2004).
 - [13] E. Matsubara, K. Yamane, T. Sekikawa, and M. Yamashita, J. Opt. Soc. Am. B **24**, 985 (2007).
 - [14] S. Akturk, C. D'Amico, and A. Mysyrowicz, J. Opt. Soc. Am. B **25**, A63 (2008).
 - [15] S. Rausch *et al.*, Opt. Express **16**, 9739 (2008).
 - [16] A.L. Cavalieri *et al.*, New J. Phys. **9**, 242 (2007).
 - [17] T. Nakajima and S. Watanabe, Opt. Lett. **31**, 1920 (2006); Phys. Rev. Lett. **96**, 213001 (2006).
 - [18] Y. Wu and X. Yang, Phys. Rev. A **76**, 013832 (2007).
 - [19] S. Chelkowski and A.D. Bandrauk, Phys. Rev. A **65**, 061802(R) (2002).
 - [20] A.J. Verhoeef *et al.*, Opt. Lett. **31**, 3520 (2006).
 - [21] D.W. Schumacher and P.H. Bucksbaum, Phys. Rev. A **54**, 4271 (1996).
 - [22] A. M. Weiner, Rev. Sci. Instr. **71**, 1929 (2000); T. Brixner and G. Gerber, Opt. Lett. **26**, 557 (2001); T. Brixner *et al.*, Appl. Phys. B **74**, S133 (2002).
 - [23] B. Xu *et al.*, Opt. Express **14**, 10939 (2006).
 - [24] NIST Atomic Spectra Database (NIST, Gaithersburg, MD) available at <http://physics.nist.gov/asd>.
 - [25] S. A. Blundell, W. R. Johnson, and J. Sapirstein, Phys. Rev. A **43**, 3407 (1991).
 - [26] M. S. Safronova, W. R. Johnson, and A. Derevianko, Phys. Rev. A **60**, 4476 (1999); M. S. Safronova and C.W. Clark, Phys. Rev. A **69**, 040501(R) (2004).
 - [27] M.S. Safronova, privet communication.

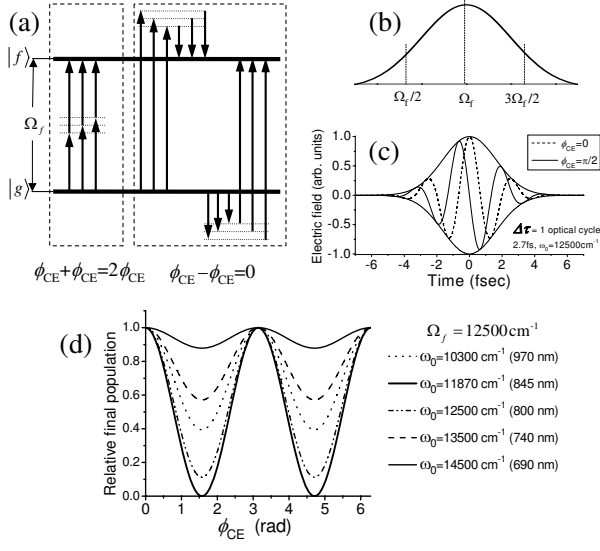


FIG. 1: (a) Two-level system excitation scheme. The two types of pathways – the sequential and the Raman pathways are indicated. (b) Ultrabroad spectrum of the single-cycle pulse. The spectrum is centered at Ω_{fg} to provide $\Omega_{fg}/2$ photons for the sequential pathways as well as $3\Omega_{fg}/2$ photons for the Raman pathways. (c) The temporal electric field of the single-cycle pulse with different CEP. (d) Degree of the two-photon absorption for the pulses with different ϕ_{CE} and different carrier frequency ω_0 , normalized to the case of $\phi_{CE} = 0$.

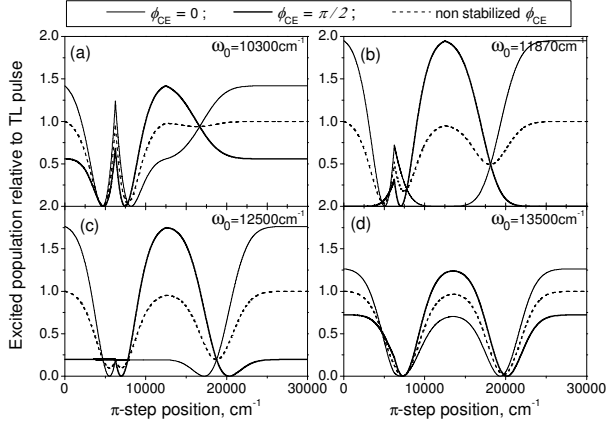


FIG. 2: Coherent control of two-photon absorption in the two-level model system. Results for a π -step phase patterns with different ω_{step} are shown for single-cycle pulses of different carrier frequencies ω_0 and different ϕ_{CE} . The two-photon absorption is normalized to the values of TL pulse with non-stabilized ϕ_{CE} .

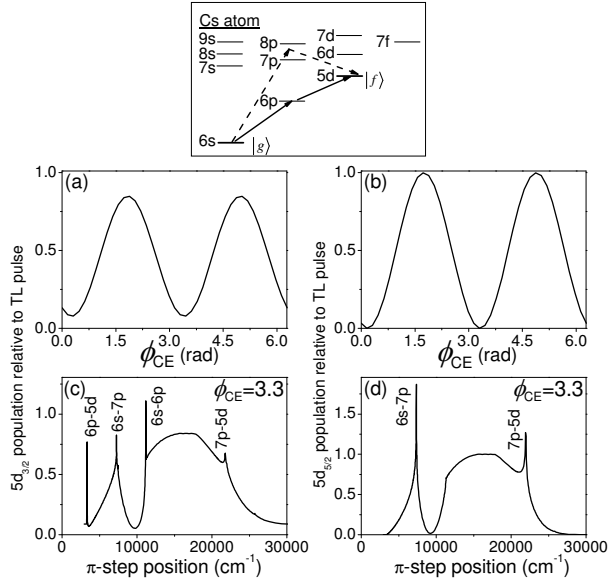


FIG. 3: Upper panel: Schematic diagram of the Cs atom (fine structure splitting is not shown). The ground state is $|g\rangle \equiv 6s$, the two excited states are $|f_1\rangle \equiv 5d_{3/2}$ and $|f_2\rangle \equiv 5d_{5/2}$. The examples of the sequential and Raman pathways are shown by solid and dashed lines respectively. Lower panel: Population of the excited states of Cs, calculated for single-cycle [fwhm=2fs] pulses with $\omega_0=16667\text{cm}^{-1}$. The results are normalized to the maximal population of the $5d_{5/2}$ state. (a),(b) The population for different values of ϕ_{CE} . (c),(d) The population excited with the phase-shaped pulses for $\phi_{CE}=3.3$. The pulses are shaped with π -step phase patterns at different ω_{step} . The enhanced transitions associated with the peaks are indicated.